The Energetic Old Age of Stars

The Effect of Late Stellar Evolution on The Structure Of the Interstellar Medium Using 1D Simulations

Juliette van der Jagt

July 14, 2020

STUDENTNUMBER	11305886
PROJECT	Bachelor Project Physics and Astronomy
SIZE COURSE	15 EC
CONDUCTED BETWEEN	01-04-2020 & 14-06-2020
INSTITUTE	Anton Pannekoek Instituut
FACULTY	Faculteit der Natuurwetenschappen, UVA & Wiskunde en Informatica & Faculteit der Bètawetenschappen / VU
SUBMISSION DATE	14-06-2020
SUPERVISORS	S. Geen & prof. dr. A. de Koter
SECOND EXAMINER	dhr. prof. dr. L. Kaper

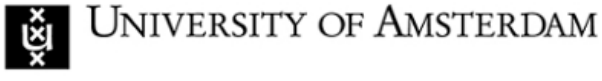

Abstract

Massive stars put out radiation and high-velocity winds during their life, that create an HII region and wind bubble in the circumstellar gas. At the end of their life their energy output changes considerably and this effects their surroundings. Using a one-dimensional hydrodynamic simulation and existing stellar tracks we study how the structure of the circumstellar gas is influenced by two highly energetic evolutionary channels. We explore the effect of a supernova and what its implications on the larger galaxy for an 18 $M_\odot$ and 100 $M_\odot$ star. Next, we look at a 12 $M_\odot$ and an 18 $M_\odot$ binary star, that loses its envelope as a result of binary interaction. Lastly, we look at the general influence of including and excluding winds in the simulation. We find that kinetic energy of the order of 10^{50} erg generated by the supernova leaves the simulation and enters the larger galaxy. The wind bubble appears to be very sensitive to recent changes in radiation and wind. We encounter complex behaviour in the wind bubble of the binary stars, that can not yet be accounted for. Lastly, we find that winds have more effect for stars with a larger mass.

Dutch summary

De vorming van sterren in ons universum is een erg inefficiënt proces. Sterren beïnvloeden hun omgeving namelijk heel sterk door het uitzenden van zonnewind en straling. We noemen de wisselwerking tussen deze twee mechanismen ook wel 'feedback'. Het begrijpen van feedback is belangrijk voor het begrijpen van het ontstaan van bijvoorbeeld sterrenstelsels maar ook voor het ontstaan van de aarde. Door de straling die de ster uitzendt ontstaat er rondom de ster een bol van geïoniseerd gas. Dit noemt men een HII gebied. De sterrenwind, die met hoge snelheid de ster verlaat, creeërt binnen in dit HII gebied een wind bubbel, waarin de dichtheid heel laag is. Aan het eind van het leven van de ster worden wind en straling velen malen sterker. Denk aan een supernova explosie, maar ook de interactie tussen dubbelsterren zorgt voor veel opschudding in de omgeving. We focussen daarom in dit onderzoek specifiek op deze situaties, die zich afspelen tijdens deze interessante tijd. Om deze complexe processen te onderzoeken versimpelen we de situatie door een ster met een gaswolk in 1D te simuleren. Het blijkt dat de wind bubbel heel gevoelig is voor hoe de ster zich gedraagt op korte termijn. Wanneer de energie van de ster vermindert, krimpt de wind bubbel snel hierna ook. Ook vinden we apart gedrag in de wind bubbel door de interactie van dubbelsterren. De simulatie laat zien dat de wind bubbel groter wordt en vervolgens krimpt. Dit is opvallend, omdat de wind en straling rond deze tijd niet veranderen. Wat de precieze oorzaak hiervan is zal meer onderzoek moeten uitwijzen. Ook vinden we dat door de supernova een kinetische energie van ongeveer 10^{43} Joule de gaswolk verlaat naar de rest van het sterrenstelsel. Als laatst, kijken we naar de invloed van het toevoegen van sterrenwind aan de simulatie. Het blijkt dat deze wind een grotere rol gaat spelen naarmate de massa van de ster groter wordt.

Contents

1 Introduction

Stars form in clouds of dense, molecular gas, that collapse under their own gravity. Due to negative feedback from young massive star clusters this process never reaches full efficiency, according to Geen et al. (2019). The stars stop accreting material, because gas is blown away with radiation, stellar winds or supernovae. As a result, the stellar masses observed in molecular clouds are smaller than what is to be expected, as explained in Geen et al. (2015). To understand this feedback mechanism a deeper understanding of the star's effect on the structure of the circumstellar medium (CSM) is desired. Stars continuously inject energy into the ambient medium and therefore change the structure of their surroundings over time. During their life massive stars emit radiation that photoionises the Hydrogen and Helium in the CSM forming spherical ionised regions around the star. These regions are called HII regions.
A lot is known today about the evolution of HII regions during the star's life. However, at the end of a star's life the energy output changes considerably in a way dictated by their evolutionary channel. Because during its life it has dispersed the cloud by radiation and stellar winds the star can in the end influence its surroundings and the rest of the galaxy more effectively than before. When stars end their life in a supernova or by losing their envelope due to binary interaction, the star's energy output increases significantly. According to Thornton et al. (1998), the evolution of galaxies and the interstellar medium are highly influenced by supernovae, which raise the kinetic energy of the interestellar medium. The effect of binary evolution can be of particular importance, as this is often left out when simulating stellar feedback, despite their large amount of ionising radiation, as discussed in Götberg et al. (2019).
In this work we look at the energy budget for how stars over their lifetime influence the CSM to understand the structure of gas clouds and the implications for the larger scale. A greater quantitative understanding of stellar feedback will allow us to gain more insight into astrophysical mechanisms such as reionisation, galaxy and star formation and galactic outflows. The evolution of the structure of the CSM is a complex process that involves a lot of physics which will be discussed in section 1.1. Including all these physical processes in a simulation would result in a more expensive simulation. In this work we try to tackle this problem by simplifying and excluding some of these processes.

We first use a simplified one-dimensional model of the star and the surrounding gas in an isolated environment and subsequently take either binary evolution or a supernova event into account. We use an existing hydrodynamic code, stellar tracks and properties of binary systems and supernovae, that are based on work from others. The specifics of the simulation will be elaborated on in section 2. We first look at these evolutionary tracks separately, after which we explore the influence of stellar winds on both cases. We try to gain more understanding of the workings of the code and possible future applications. Also this research does not look much into implications for the rest of the galaxy, but is an interesting topic for future research.
We start by discussing the specifics of a typical HII region, binary evolution, supernovae and stellar winds in section 1.1. Then we describe the workings of the hydrodynamic simulation in section 2. In addition, the stellar evolution models that are used are presented here. Following this the results from the simulation are presented in section 3. In section 4 the results are placed into a wider context and anomalies are elaborated on. Finally, in section 5 we summarize our findings.

1.1 HII region

In figure 1 a schematic of a typical HII region and wind bubble is shown. The following description is based on Dyson (1977).

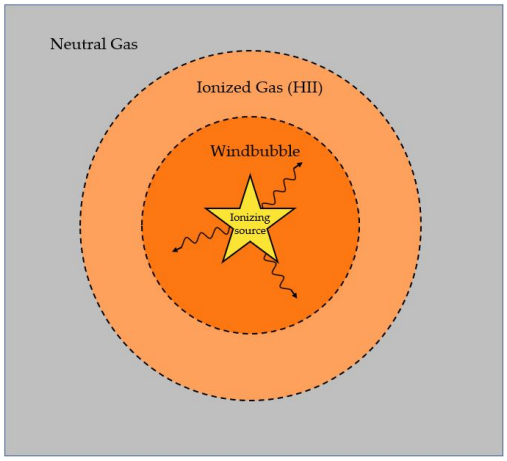

Figure 1: Schematic showing of an HII region consisting of sphere of ionised gas and a wind bubble around a star with ionising radiation. The HII region is surrounded by neutral gas.

Massive stars emit high-energy UV radiation, which is able to ionize the surrounding hydrogen. The star becomes surrounded by a sphere of ionised gas, the HII region, which will start to expand outward once

the temperature and thus the pressure of the ionised material is high enough. The warm gas shocks against the cold neutral background, creating an ionisation front. As the ionisation front expands, it pushes away the neutral gas. This yields in a neutral dense shell with a low-density, ionised region on the inside and low-temperature, high-density gas on the outside.
A similar process driven by stellar winds instead of radiation takes place inside the HII region. Gas leaves the star with a temperature similar to the surface temperature and travels with a speed of the order of the star's escape velocity. These high-velocity winds shock with the ionised gas creating a sphere of hot gas due to the thermalisation of kinetic energy, the wind bubble. Around the star also forms a free-streaming radius driven by these fast flows, as stated in Weaver et al. (1977). The winds have not yet shocked with the background, which is the case for the thermalised part of the wind bubble.
In figure 2 a typical density profile of an HII region is shown. The wind bubble is very under-dense and is separated by a shock front from the denser HII region, which is surrounded by a dense shell. The wind bubble and HII region can be distinguished by their temperature which are of the order 10^4 and 10^8 K, respectively. This shell is neutral, just like the ambient medium.

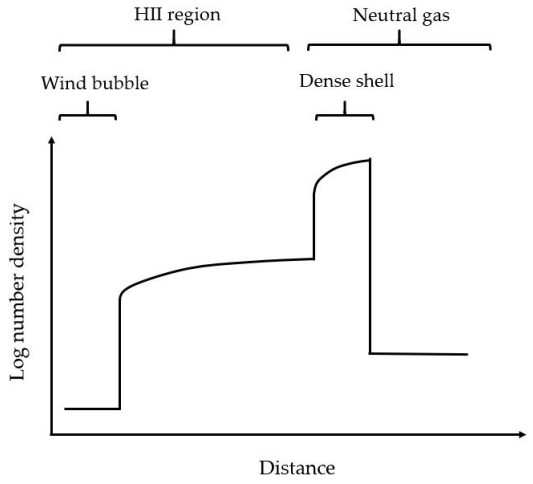

Figure 2: Schematic showing of the density profile of an HII region. Figure adapted with permission from Geen et al. (2019). Original from Rahner et al. (2017)

The expansion of the HII region can be divided into two phases, as described by Geen et al. (2015). In the first phase the HII region radius reaches the Strömgren radius. Inside this radius the number of recombinations and ionisations cancel eachother out. This radius can be calculated by

$$r_{st} = \left(\frac{3}{4\pi} \frac{Q_H}{n_i n_e \alpha_B} \right)^{\frac{1}{3}}, \tag{1}$$

where Q_H is the flux of the ionising photons from the the star in photon per unit time, n_i and n_e are the ion and electron number density and α_B the recombination rate of the photoionised gas. In the second phase the expansion is due to the thermalisation by photoionisation. The analytic description is provided by the Spitzer solution:

$$r_i = r_{st} \left(1 + \frac{7}{4} \frac{C_i t}{r_{st}} \right)^{\frac{4}{7}}, \tag{2}$$

where C_i is the speed of sound in the ionised gas ($\simeq$ 100 km/s) and r_i is the radius of the HII region. (Spitzer, 1978)

1.2 Stellar evolution

Stars are powered by nuclear fusion in their core during their life. For massive stars this fusion lasts a time of the order of 10 Myr, after which they burn through their hydrogen supply. Their core collapses and the outer layers are blown away. The way stars end their life is dependent on the mass and dominant processes acting on their structure, as discussed in Heger et al. (2003). Stars with masses above 8-10 $M_\odot$ can end their life in a supernova event. When stars are part of a binary system their smaller companion can strip away their hydrogen rich shell. In the following sections both cases will be discussed, after which we will look closer into stellar winds.

1.2.1 Binary evolution

Two stars can be part of the same star system in which they rotate around their common center of gravity. The most massive star runs out of its hydrogen supply faster than its smaller companion and swells up. When this happens the smaller secondary can strip away the envelope of the primary star, because the gravitational pull from the secondary becomes greater than that of the primary, as described by Götberg et al. (2019). This process increases the energy output of the star system. According to Sana et al. (2012), massive stars are often part of a binary systems and 40-50 % get stripped from their envelope. The number of ionising photons emitted by stripped stars is significantly larger than for regular massive stars, as stated in Maxwell & Stefano (2017).

1.2.2 Supernovae

A star can end its life via a supernova, a very luminous explosion where the star releases a large amount of energy instantaneously. Supernovae are the major driving force in the distribution heavy elements to the interstellar medium, as stated in Thornton et al. (1998). They are a dominant source for the kinetic energy in gas clouds and have therefore also a big influence on later star formation. This subsequently has influence on the number of supernovae in the galaxy.

1.2.3 Stellar winds

During the star's life it loses material in continuous streams which move with the star's escape velocity away from the star. These high-velocity winds transfer kinetic energy to the CSM. As described in section 1.1, these high-energy stellar winds can create a wind-driven bubble around the star. The mass loss rate and wind luminosity is dependent on the stage in the life the star is in.

2 Methods

We use existing stellar tracks and an existing hydrodynamics code to simulate the stellar source and the CSM. We implement binary evolution data and the properties of supernovae to simulate the end of the star's life. We also modify the code so that the temperature of the ionised gas is implemented into the simulation. Supernovae are simulated for a 18 $M_\odot$ and a 100 $M_\odot$ single star, which is explained in section 2.5 and binary evolution is simulated for a 12 $M_\odot$ and an 18 $M_\odot$ binary star, as explained in section 2.6.

2.1 Hydrodynamic code

Our goal is to model a star and the surrounding gas in a closed environment so all influences from outside sources, such as heating or winds are neglected. The one-dimensional hydrodynamic simulation code is available on Github[1]. It integrates VH-1, a hydrodynamics code written in FORTRAN and includes cooling, radiation and winds, which will be discussed in the following sections separately. The gas is treated as ions, electrons and neutral atoms instead of distinguishing each elements. For each simulation 256 cells are distributed over a grid representing an area, which maximum radius is dependent on the stellar source. It needs to be wide enough to include the expansion of the HII region, but small enough to preserve the resolution. At each moment in time the forces on the cells are calculated and mass is either moved to or added from a neighbouring cell. The first cell of the grid represents the stellar source. The properties for this source were retrieved as described in section 2.2. The metallicity of the gas is set to solar metallicity (Z = 0.014). Self gravity was not taken into account, because self gravity is not a strong force for these structures as they are more or less spherically symmetric, as explained by Geen et al. (2015).

[1] https://github.com/samgeen/Weltgeist.git

2.2 Star simulation

To simulate the stellar source we use the method described by Geen et al. (2019) in which they calculate the spectra using STARBURST99 from Leitherer et al. (2014). The original tracks are given by the Geneva tables generated by Ekström et al. (2012). These tracks represent the typical behaviour of non-interacting rotating stars. By interpolating linearly between the information from different stellar masses they retrieve values for the ionising photon emission rate, wind luminosity and wind mass loss during the star's life. They determine the temperature of the ionised gas by using Cloudy (Ferland et al., 2017) and the star's effective temperature. Because the different atoms in the gas are not distinguished, the temperature of the ionised gas is set to a higher value around hotter stars.

2.3 Radiation

To simulate the radiation a simple ionisation/recombination model is used. A ray is traced through the spherical grid and ionises everything it passes. The assumption was made that the ionised gas is in photoionisation equilibrium, which is satisfied by

$$\frac{4\pi}{3} r_i^3 n_i^2 \alpha_B = Q_H, \tag{3}$$

Note that this is equation 1 rewritten. α_B is approximated by using the recombination rate for only hydrogen, which is calculated as

$$\alpha^B_{HII} = 2.753 \times 10^{-14} \frac{\lambda_{HI}^{1.503}}{[1 + (\lambda_{HI}/2.74)^{0.407}]^{2.242}} \tag{4}$$

in Rosdahl et al. (2013), Appendix E2. λ_{HI} is a unitless function defined as

$$\lambda_{HI} = \frac{315\,614\,K}{T}, \tag{5}$$

where T is the temperature in K.

2.4 Cooling

The cooling is related ρ^2, where ρ is the density, because most cooling channels are caused by collisions. If the number of particles in a volume increases by a factor of 2, the chance that they collide increases by a factor of 4. To simulate the cooling the method the code adopts the method of Audit & Hennebelle (2005). The dominant physical processes are cooling by fine-structure lines of CII and OI, the Lyα line of H and electron recombination onto positively charged grains. Regarding the molecular properties of the gas we assume γ = 5/3 for a monatomic gas.

2.5 Supernova

The stellar tracks are used to simulate the star up to the end of its life. After this the stellar source is replaced by the properties of the supernova. The released kinetic energy of the supernova is approximated 10^{51} erg and the ejecta by 1 $M_\odot$ for both stars, as used in Geen et al. (2018). The maximum radius of the grid is of 27 pc and 35 pc for the 18 $M_\odot$ and 100 $M_\odot$ star simulation, respectively. It should be noted that the 100 $M_\odot$ might not even go supernova. According to Heger et al. (2003), for stars with a mass bigger than 25 $M_\odot$ this is dependent on the mass and their metallicity. Very massive low metallicity stars are likely to transform into a black hole with no or a small supernova prior to that.

2.6 Binary stars

Binary evolution is complicated and taking into account the possible scenarios of binary interaction is far beyond the scope of this report. To simulate the stripped star the spectral and evolutionary models from Götberg et al. (2019) were used. They calculated the ionising photon emission rates, mass loss rates and wind luminosity for primaries in a binary system with initial masses of M_{init} = 12.17 $M_\odot$ and M_{init} = 18.17 $M_\odot$. These stripped stars are created through Case B mass transfer, which means they are stripped from their envelope relatively early before they burn through their hydrogen supply. According to Götberg et al. (2019), this evolutionary channel is the most common. Therefore it is sufficient for the purpose of this study. The radiation and winds emitted by the smaller companion are neglected, because the radiation output of this star is significantly smaller compared to their primary. The 18 $M_\odot$ and 12 $M_\odot$ stars lose their envelope at 10.7 Myr and 18.8 Myr, respectively, leaving behind a 6 $M_\odot$ and 4 $M_\odot$ star. The stripped envelope phase lasts 0.8 Myr for the 18 $M_\odot$ star and 1.5 Myr for the 12 $M_\odot$ star. The total ionising photon emission rates are $\log(Q_{H,18M_\odot})$= 48.7 and $\log(Q_{H,12M_\odot})$= 48.1 with mass loss rates of $\dot{M}_{18M_\odot}$= 2.20 × 10^{21} g/s and $\dot{M}_{12M_\odot}$=1.89 × 10^{20} g/s and with velocities of $v_{inf,18M_\odot}$ = 2570 km/s and $v_{inf,12M_\odot}$ =2100 km/s. The maximum radius of the grid is 27 pc for both sets of simulations.

2.7 Winds

To get more insight into the physical influence of winds, all simulations are performed with and without stellar winds. Because these winds move so fast, the simulation is bound to the Courant limit. The Courant condition states that the time step must be small enough so that all the physical information from the previous time step is still included. Gas can not travel faster than this time step. Thus when these fast winds are included into the simulation the simulation time goes up significantly.

3 Results

In this section the results of the simulations are presented. We start by comparing the simulation to the analytic Spitzer solution and show how the HII region and wind bubble radius, kinetic energy, thermal energy and momentum evolve over time. We briefly review the general structure of the gas during the life of the stars. Following this we focus on the structure of the HII region and wind bubble at late times and the influence of supernovae and binary interaction.

3.1 Simulation accuracy

To give an indication of the accuracy of the simulation the analytic Spitzer solution is compared to the hydrodynamic simulation. The Spitzer solution, equation 2, gives an approximation to the radius of the ionisation front for a constant radiation source. This constant radiation source is approximated by extracting the maximum ionising photon rate during the star's life from the stellar track, which take the value of $Q_{H_{max},18M_\odot}$= 2.32e48 s^{-1} and $Q_{H_{max},100M_\odot}$ 1.20e50 s^{-1}. The 12 $M_\odot$ is left out as the stellar tracks for the 12 $M_\odot$ and 18 $M_\odot$ are very similar. To make a fair comparison, the only source in this simulation is the constant value for radiation and winds are left out. In figure 3 both the analytic solution and the simulation are shown and we can see how there is a small divergence in the radius of the 18 $M_\odot$ star at late times and the radius of the 100 $M_\odot$ diverge in the beginning and end. This deviation will be discussed

further in section 4. For the 100 $M_\odot$ star the HII region first expands to the Strömgren radius, which is the point where recombination and ionisation are balanced as described by equation 1. For the 100 $M_\odot$ star this radius equals 7 pc.

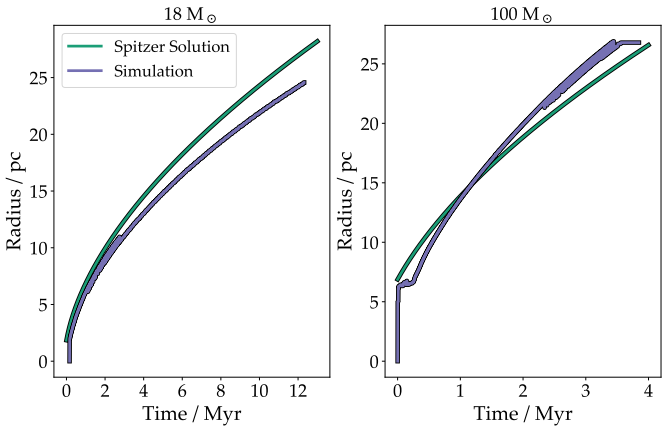

Figure 3: The analytic Spitzer solution compared to the one-dimensional hydrodynamic simulation both calculated or simulated at constant ionising photon emission rates, which are $Q_{H_{max},18M_\odot} = 2.32e+48\ s^{-1}$ and $Q_{H_{max},100M_\odot} = 1.20e50\ s^{-1}$.

3.2 The structure at early times

The evolution of the structure of the CSM is very similar for the different stars modelled in this report. Therefore, the 18 $M_\odot$ star will be used to discuss the general structure of the gas. Snapshots of the radial profiles for the number density and temperature are shown in figure 4 and correspond to 1.0 Myr, 5.0 Myr and 9.0 Myr into the life of the star. From the figure the HII region and wind bubble are identified as the areas with temperatures above 10^4 K and 10^8 K, respectively. On the edge of the HII region the dense shell is visible as the spike in the density and a drop in temperature. These regions expand to a larger radius over time.

3.3 Supernova

The simulations including a supernova will be presented here and we will look at the behaviour of the HII region and wind bubble before and after the supernova event. The simulations are generated by using the stellar tracks until the end of the star's life. These properties can be found in the Appendix in figure 16 and figure 17. After that the supernova properties as mentioned in section 2.5 replace the stellar source.

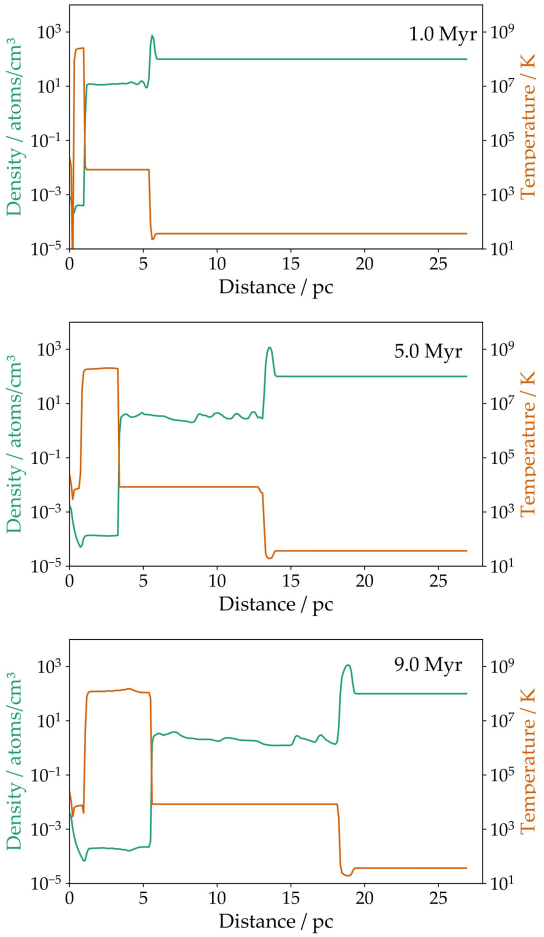

Figure 4: The number density and temperature radial profiles at times t = 1.0 Myr, 5.0 Myr, 9.0 Myr for an 18 $M_\odot$ star.

The radii, momentum and kinetic energy in the HII region, wind bubble and total gas are shown as function of time for the 18 $M_\odot$ star in figure 5 and for the 100 $M_\odot$ in figure 6. The HII region and wind bubble radius are calculated by sampling the temperature of the gas. The wind bubble is in both cases overtaken by the supernova blastwave which reaches the edge of the HII region, where further expansion is obstructed by the ambient medium. The wind bubble of the 100 $M_\odot$ star reaches much further to edge of the ionised region, which can be due to a smaller ratio of wind luminosity to ionising photon emission rate in the 100 $M_\odot$ star. In the plot for kinetic energy both stars show how the kinetic energy of all the gas in the grid is higher by one order of magnitude compared to the kinetic energy in the HII region. This indicates that most of the kinetic energy

is in the dense shell, as the almost static neutral gas has a very low kinetic energy. After the supernova event the kinetic energy in the HII region and wind bubble decrease, because the supernova blast wave has destroyed the HII region and wind bubble and left behind a low-density, hot supernova remnant. The fluctuations in the kinetic energy of the HII region and wind bubble are caused by a combination of sound waves and small sampling errors in the way the stellar properties are extracted by interpolation. Right before the supernova event the wind bubble collapses. The possible causes for this outcome will be elaborated on later in section 3.5.

3.4 Binary system

The simulation for the binary system uses the star properties from the stellar track to the point the star loses its envelope, after which the properties of the stripped envelope are implemented. The star's effective temperature and temperature of the ionised gas are shown in figure16 and the total photon emission rate, wind luminosity and wind mass loss are shown in figure 17. These figures can be found in the Appendix. The total photon emission rate includes all ionising photons for HII, HeII and HeIII. To get an idea of the difference in the density profile between the simulation for the binary star and the single star, a snapshot is shown for the 18 $M_\odot$ star at

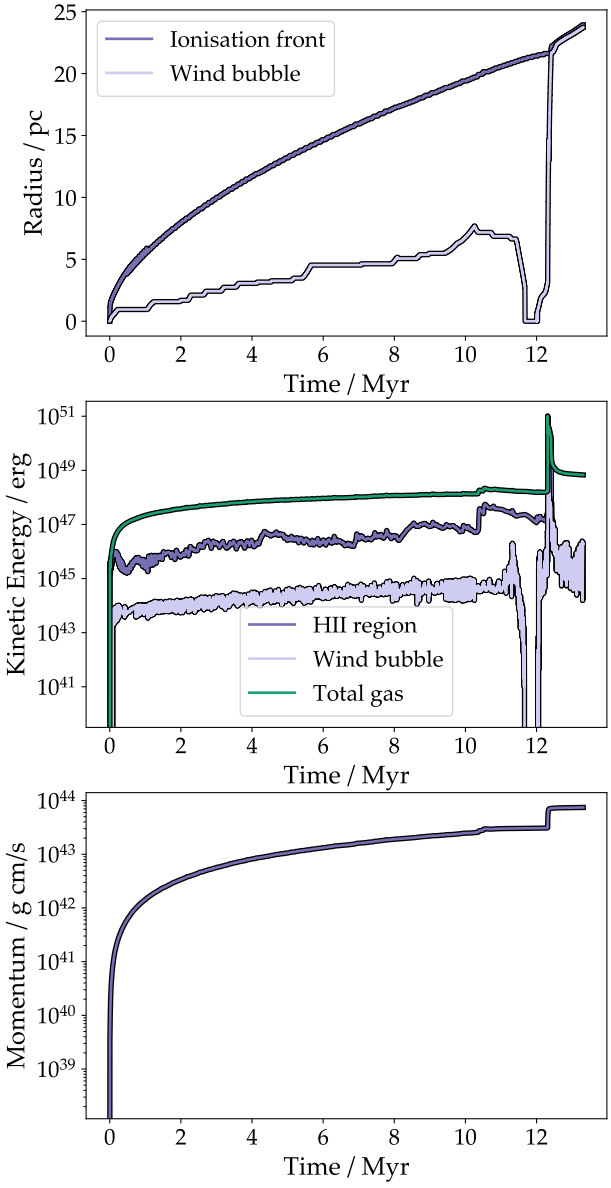

Figure 5: HII region and wind bubble radius, kinetic energy and momentum as function of time for the 18 $M_\odot$ star that ends its life in a supernova.

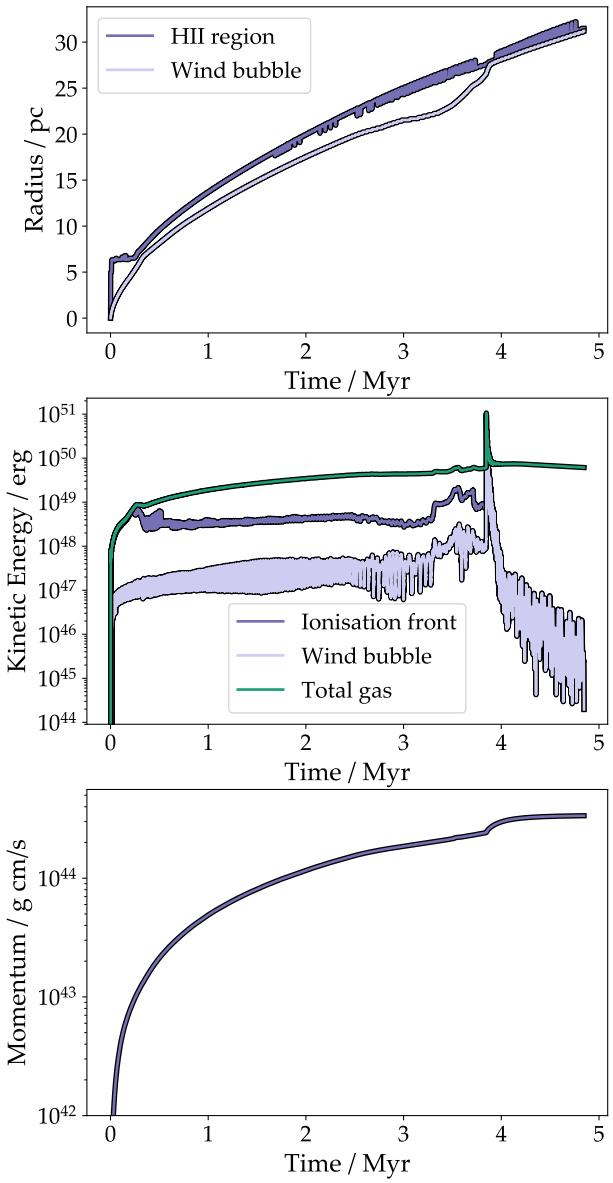

Figure 6: HII region and wind bubble radius, kinetic energy and momentum as function of time for the 100 $M_\odot$ star that ends its life in a supernova.

11.5 Myr for both cases in figure 7. Although there is no difference in the expansion of the HII region, the wind bubble of the binary star has expanded significantly compared to the single star. In the snapshot for the binary star the free- streaming radius takes up about half of the wind bubble. In the HII region the density is higher and the temperature is of the order of 10^4 K, while the temperature in the thermalised region of the wind bubble is 10^8 K. When we look at the radius as function of time it becomes more clear how the HII region and wind bubble evolve at the end of the stars life. In figures 9 and 8 the binary and single star evolution are shown for the 12 $M_\odot$ and 18 $M_\odot$ stars. The change in radiation and winds caused by stripped envelope of the 18 $M_\odot$ star merely influences the wind bubble while for the 12 $M_\odot$ star both the wind bubble and HII region expand more when the star loses its envelope. However, the wind bubble shrinks after 19.0 Myr. Also the wind bubble of the 12 $M_\odot$ and 18 $M_\odot$ single star collapse. The structure of the wind bubble for both situations will be discussed more extensively in section 3.5.

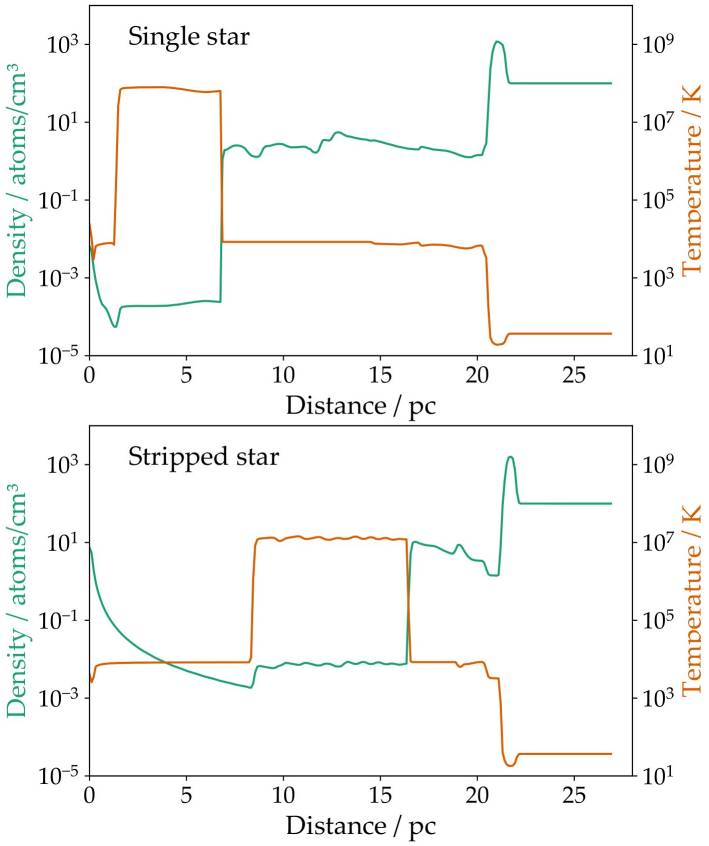

Figure 7: the number density and temperature profile at 11.5 Myr for the 18 $M_\odot$ star. The top plot shows the end when the star is stripped from its envelope. The bottom plot show the end for the single star.

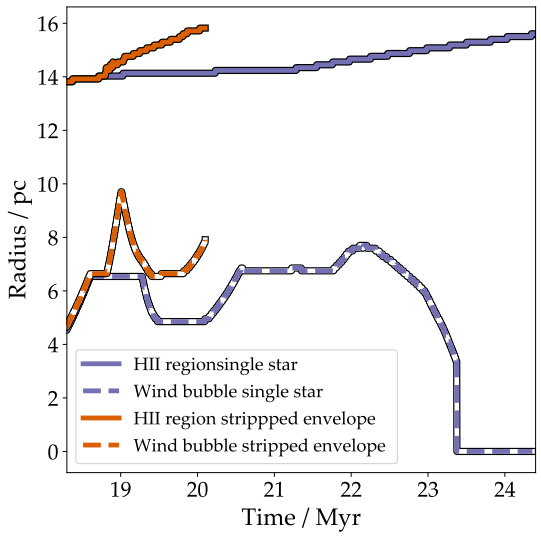

Figure 8: The radius of the wind bubble and ionisation front as a function of time for the 12 $M_\odot$ star. The orange line shows the radius for the stripped star that loses its envelope at 18.8 Myr. The purple line shows the radius for the single star.

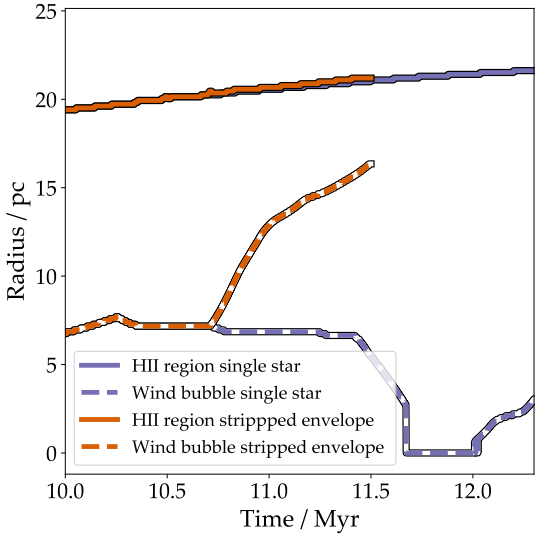

Figure 9: The radius over time of the wind bubble and HII region for the 18 $M_\odot$ star. The orange line shows the radius for the stripped star that loses its envelope at 10.7 Myr. The purple line shows the radius for the single star.

3.5 Structure of the wind bubble

In the previous sections we encountered an anomaly in the evolution of the wind bubble. At later times there is a collapse in the wind bubble of the 12 $M_\odot$ and 18 $M_\odot$ single stars and a decrease in the wind bubble of the 12 $M_\odot$ binary star. Interestingly, the wind bubble does collapse for the 18 $M_\odot$ binary star and the wind bubble of the 100 $M_\odot$ only experiences a relative small decrease. By looking at snapshots during the collapse we attempt to acquire more insight. In figure

10 the number density and temperature profile are shown for the 12 $M_\odot$ single star at times 19.0 Myr, 19.4 Myr and 20.0 Myr. The wind bubble contracts in the time between 19.0 Myr and 19.4 Myr and expands again after 19.4 Myr. The snapshot at 19.4 Myr shows that the density just outside the edge of the wind bubble increases and when the density increases, the recombination rate goes up. It turns out that the ionised region indeed decreases to the radius of the wind bubble. The ionisation front lines up with the edge of the wind bubble, which reveals that the ionising photons are trapped by the material that is pushed away by the wind bubble.

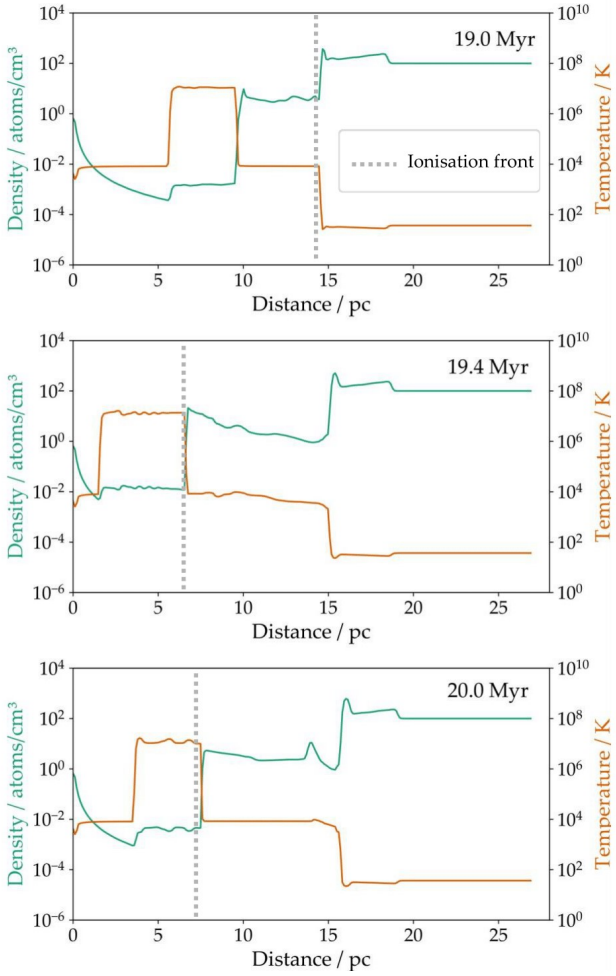

Figure 10: Snapshots of the number density and temperature radial profile of the 12 $M_\odot$ single star for times 19.0 Myr (top), 19.4 Myr (middle) and 20.0 Myr (bottom). The Ionisation front is represented by the dotted grey line.

In figure 11 the density and temperature profile are shown for the 12 $M_\odot$ single star at 21.0 Myr, 22.5 Myr and 24.0 Myr. These times correspond to two moments before the collapse and one after. We can see how the lower dense, high temperature region disappears over time, while the HII region remains unchanged.

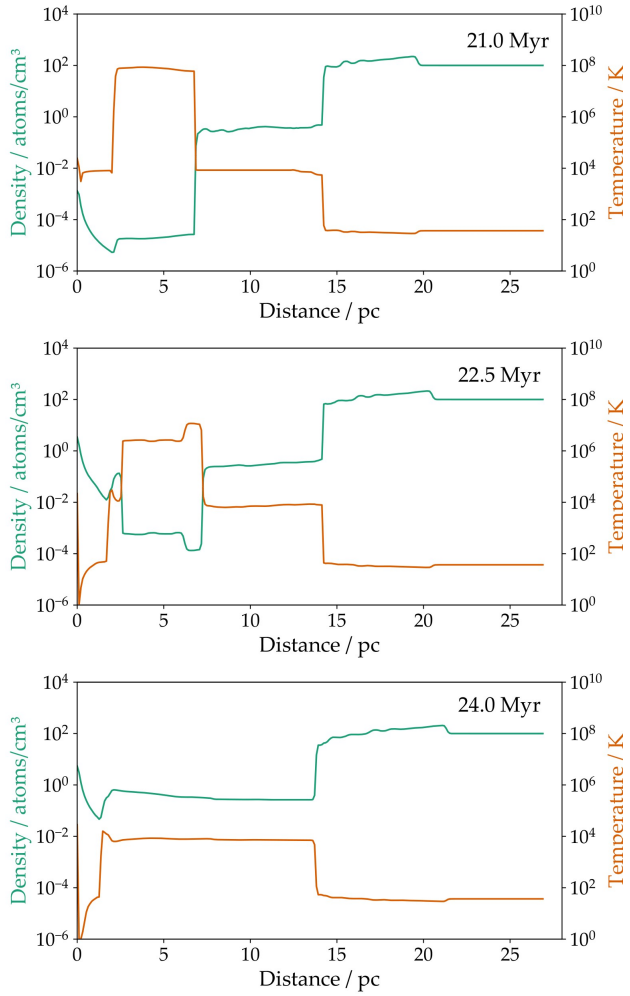

Figure 11: Snapshots of the number density and temperature profile of the 12 $M_\odot$ single star for times 21.0 Myr (top), 22.5 Myr (middle) and 24.0 Myr (bottom).

To get more understanding of the collapse of the wind bubble at late times for the two binary stars we focus on the connection between the wind and radiation output of the star and the energy in the wind bubble. Figure 12 shows the energy of the wind bubble, the wind luminosity and total photon emission rate for both binary stars. For both the energy inside the wind bubble collapses around 1 Myr after the wind luminosity and total photon emission rate also collapse. Looking at the 18 $M_\odot$ star, the radiation and wind luminosity increase again around 12 Myr to which the energy of the wind bubble responds in the same way as before. The fluctuation in energy of the wind bubble seems to be a direct results from the fluctuation in radiation and wind. The wind luminosity and ionising photon emission rate of the 100 $M_\odot$ star do not show this fluctuating behaviour. The wind bubble of this star also does not collapse. A hypothesis of the behaviour of the wind bubble will be presented in section 4.2.

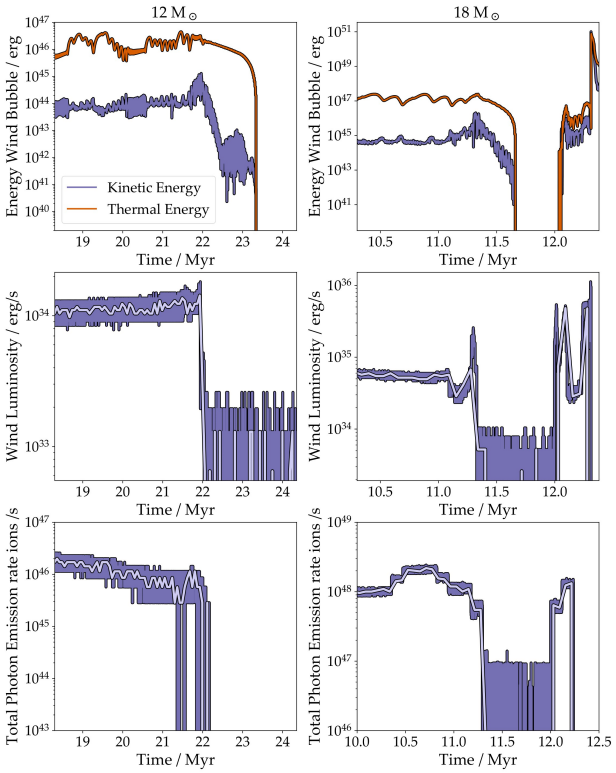

Figure 12: The energy of the wind bubble, wind luminosity and total photon emission rate for the 12 $M_\odot$ star from 18.5 Myr (left) and 18 $M_\odot$ star from 10.3 Myr (right). The wind luminosity and total photon emission are plotted for the time step corresponding to the simulation in purple and a bigger time step of 0.025 Myr in light purple.

There appears to be a lot of numerical noise in the wind luminosity as well as in the total photon emission rate when the time step of the simulation is used to extract these properties from the stellar tracks. To show how the radiation and winds behave on average the wind luminosity and photon emission rate are both generated by using a bigger time step of 0.025 Myr. By using this bigger time step the level of fluctuations is diminished.

3.6 Influence of wind

In this section we will look at the influence of winds on the expansion and energy of the HII region and wind bubble. In figure 13 the HII region radius and wind bubble radius are shown for when winds are included and excluded for the 100 $M_\odot$ and 18 $M_\odot$ single star. There is a very small difference in the HII region radius for the 18 $M_\odot$ star, but for the 100 $M_\odot$ this difference is significantly bigger. To clarify this, in figure 14 the difference in radius between the simulations that includes winds and excludes winds is plotted as function of time. This is done for the 12 $M_\odot$, 18 $M_\odot$ and the 100 $M_\odot$ star without including the supernova event or binary interaction. The HII region radius for the other 12 $M_\odot$ and 18 $M_\odot$ stars is not shown separately, because the difference is very small and similar to the 18 $M_\odot$ supernova star, which is the star that ends in a supernova.

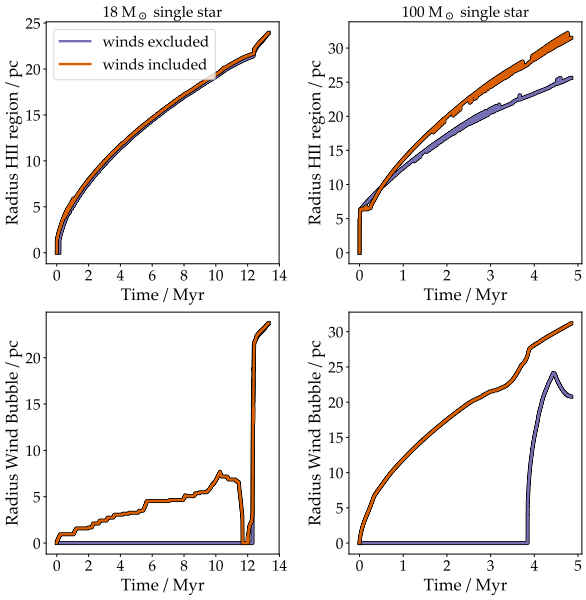

Figure 13: The HII region radius and the wind bubble radius when winds are included and excluded for the 18 $M_\odot$(left) and the 100 $M_\odot$ single stars (right) with a supernova at the end of their lives. The supernova event happens at 12.4 Myr for the 18 $M_\odot$ star and at 3.8 Myr for the 100 $M_\odot$ star, after which the wind bubble radius becomes the supernova remnant.

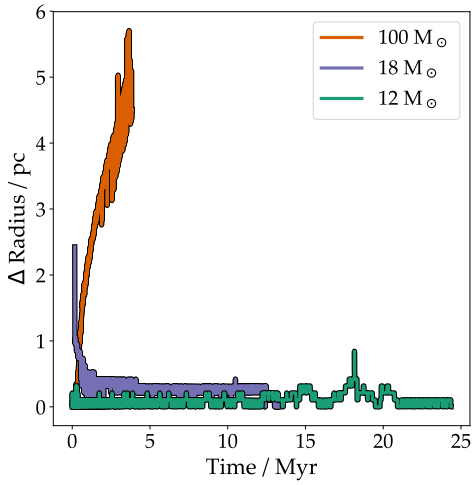

Figure 14: The difference in HII region radius between the simulation with winds included and winds excluded for the 12 $M_\odot$, 18 $M_\odot$ and the 100 $M_\odot$ star.

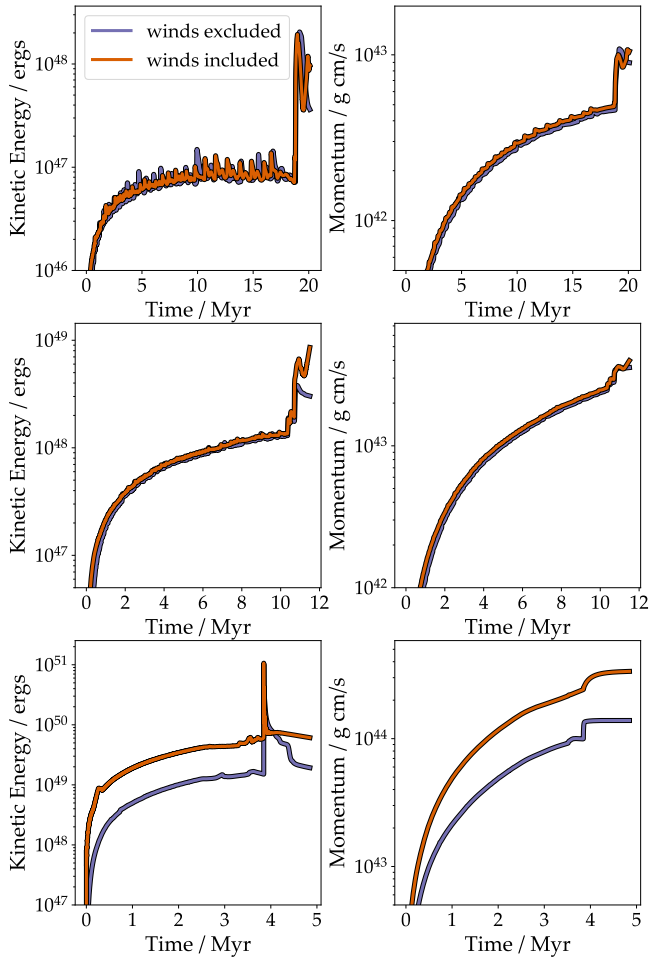

Figure 15: Kinetic energy and momentum when winds are included and excluded for the 12 $M_\odot$ and 18 $M_\odot$ binary stars (top and middle) and the 100 $M_\odot$ supernova star (bottom).

Figure 15 shows the kinetic energy and momentum for the 12 $M_\odot$ and 18 $M_\odot$ binary stars and the 100 $M_\odot$ supernova star. The 18 $M_\odot$ supernova star is left out, because the main life of the star is the same as the 18 $M_\odot$ star and the difference in kinetic energy and momentum during and after the supernova is very small. During the life of the binary stars the difference is also very small. When the star is stripped from its envelope there is a small deviation in kinetic energy for the 18 $M_\odot$ binary star. We can also notice how the kinetic energy fluctuates when winds are included, but decreases slowly when winds are absent and that this fluctuation is bigger for the 12 $M_\odot$ star. This could be linked to the apparent behaviour of the HII region and wind bubble radii as described in section 3.5, but this will be discussed further in section 4.2. For the 100 $M_\odot$ star the kinetic energy increases when the supernova event happens at 3.8 Myr for both simulations. After this the kinetic energy stabilises to the value it had prior to the supernova event.

4 Discussion

In this section the most important results will be placed in a larger context to reveal their significance. The structure of the results section is maintained. First, the difference between the analytic solution and the simulation is reviewed. We discuss the sensitivity of the wind bubble and suggest a physical explanation, after which we look into the influence of winds. Finally, we briefly review the implications on a larger scale and suggest what could be done for future research.

4.1 Analytic solution

As presented in section 3.1 there is a deviation between the analytic solution and simulation. It should be noted that the Spitzer solution does not include all the physics that are involved. For example, the HII region of the 100 $M_\odot$ star first expands to the Strömgren radius and causes the analytic solution and the simulation to be different in the beginning. Moreover, according to Rosdahl et al. (2013) the Spitzer is not really suited for validating numerical simulations. They found a significant deviation between twelve numerical simulations and the Spitzer solution. Bisbas et al. (2015) generated a different formula that is more appropriate for validating numerical simulations, which will be used to test the code before future publication.

4.2 The sensitivity of the wind bubble

For the 12 $M_\odot$ and 18 $M_\odot$ single stars the wind bubble totally collapses at late times. By looking at the relation between the energy inside the wind bubble and the radiation and wind output of the star we find that the two strongly correlate. The energy in the wind bubble collapse as a response to the collapse in the energy output of the star. This collapse is absent for the HII region radius, but the principle of cooling in the wind bubble can help explain this behaviour. The wind bubble has a much lower density than the ionised region due to pressurisation of highly kinetic particles, that are a result of the high-velocity winds. When this pressure decreases the bubble shrinks, which causes the gas to mix more and also increase the cooling. When cooling is more efficient, the

temperature will decrease more rapidly and pressure will decrease faster, resulting in a collapse in the radius of the region. The wind bubble thus reacts much faster to changes in wind and radiation than the ionised gas.
The collapse of the wind bubble is an important result to understand the sensitivity to recent stellar evolution. This implies that the nebula reflects the star's behaviour in the last few million years of its life. This understanding can also be a relevant in the process of translating observational data into measurements. A similar sensitivity of the wind bubble to fluctuations in wind luminosity and ionising photon emission rate was also found by Geen et al. (2015).
It should be noted that there is a possibility that the cooling is overestimated. According to Pabst et al. (2019) the Orion nebula cools very inefficiently, while simulations would predict winds cool very efficiently. If this is the case, the wind bubble might react less strong to changes in the star's radiation and wind. This calls however for more physics and a better resolution. In section 3.5 we argue that for the 12 $M_\odot$ binary star and 18 $M_\odot$ single star the ionising photons get trapped inside the wind bubble. This phenomenon is sometimes found in physical HII regions, such as the Orion Nebula like Pabst et al. (2019) found. However this nebula is much younger. For the 12 $M_\odot$ binary star it is very paradoxical that ionising photons get trapped at the time radiation and winds become a lot stronger. Also, the HII region does expand, even though these photons are trapped by the wind bubble. For the single stars is found that the wind bubble responds very specific to the fluctuations in wind luminosity and ionising photon rate. Based on this finding the wind bubble of the 12 $M_\odot$ binary star is not expected to fluctuate, as the wind luminosity and radiation are constant. Future research must point out what mechanism is really causing this.

4.3 The role of winds

The effect winds have on the simulation increases when the mass of the star is higher. This is due to the fact that stars with a higher mass have stronger winds. We can conclude the difference in wind is mostly due to the strong wind luminosity during the star's life, as the energy released by the stripped envelopes and supernovae do not cause the simulations to differ significantly. Radiation seems to be the driving force in the expansion of the HII region and winds play a significant role only for very massive stars. This dominant influence of photoionisation was also found by Krumholz & Matzner (2009) and Capriotti & Kozminski (2001), who stated that winds were indeed less significant. To determine a boundary for when winds become important more stars must be simulated in the same way. Winds may play a role in the complex behaviour of the HII region and wind bubble radii for the binary stars. When winds suddenly become stronger, which is the case when the star is stripped from its envelope, the wind bubble needs time to restore pressure balance. When winds are included the kinetic energy of the total gas fluctuates after the star looses its envelope. This can indicate that the decrease is indeed caused by the pressure balance that is not yet reached. However, from the current results it does not become apparent what the cause is and we therefore need more insight by further research.

4.4 Consequences for the galaxy/large scale

To say something about the energy transfer caused by supernovae, we compare the energy injected by the supernova and how much is transferred to the gas. The final kinetic energy of the total gas is of the order the 10^{49} erg compared to an energy input of 10^{51} erg. We see not all kinetic energy remains in the gas 1 Myr after the supernova event. Energy of the order of 10^{50} erg is leaving the gas in the simulation and creating turbulence in the galaxy or escaping the galaxy all together.

4.5 Future research

In this study some physics that could be important is left out for simplification. In a follow-up study either the importance of these mechanisms can be studied using the hydrodynamic code or some physics can be added to improve the approximation of reality. The recombination rate of only hydrogen was used. To get a more accurate value, one could also implement the recombination rates of HeII and HeIII. The simulation also did not include self gravity, but this should be considered in future work, as it might have an effect on the dense shell.
Also, the Geneva tables also provide stellar tracks for non-rotating stars. This code can be used to see if there is a difference between the influence of rotating and non-rotating stars. Other physics that can be included is radiation pressure, or exploring the effect of changing parameters such as metallicity and density of the ambient medium. In section 3.5 it is shown how there is noise present in the stellar properties, because of the way the properties are extracted from the stellar tracks by interpolation

between different stellar tracks. In a follow-up study the stellar evolution tables should be updated to reduce this noise. More insight into large scale galactic effects would be an interesting topic for further research. One could examine when the dense shell becomes unstable. When this happens, the shell can fragment and new star formation can take place.

5 Conclusion

The results of a study are presented in which we look into the evolution of the CSM for 12 $M_\odot$ and 18 $M_\odot$ binary stars and 18 $M_\odot$ and 100 $M_\odot$ stars that end their life in a supernova. We find that the wind bubble is very sensitive to recent stellar evolution. Efficient cooling in the wind bubble could be causing this, but it also a possibility cooling is overestimated. We find a lot of noise in the extracted stellar properties. This needs to be updated in future research. Other anomalous behaviour was found in the wind bubble of the 12 $M_\odot$ binary star. Ionising photons get trapped inside the wind bubble, even though radiation and winds are stronger. There is a possibility that pressure equilibrium is not yet reached and as a result the wind bubble collapses. A full understanding of what drives the behaviour of the wind bubble radius requires more research. Radiation seems to be the driving force in the expansion of the HII region and winds play a significant role only for very massive stars of around 100 $M_\odot$. Stellar winds have more effect on stars with a higher mass. This is probably due to the fact that stars with a higher mass have a higher wind luminosity. The final kinetic energy of the total gas is of the order the 10^{49} erg compared to an energy input of 10^{51} erg for the simulations that included a supernova event. This energy is transferred to larger scales in the galaxy, where it will drive turbulence or escape the galaxy all together.

6 Acknowledgements

Thanks go out to Sam Geen for giving me the opportunity to work with the code he wrote and for sharing his knowledge and supervision, that ensured the success of this project. Thanks go out to Ylva Gotberg for sharing her data and knowledge of binary evolution and thinking along with this study. Finally, I would like to thank the Stars and Stellar Populations group at API for giving interim suggestions for the project and for making me feel welcome in their research group.

Bibliography

Audit E., Hennebelle P., 2005, Astronomy and Astrophysics, 433, 1, Thermal condensation in a turbulent atomic hydrogen flow

Bisbas T. G., et al., 2015, Monthly Notices of the Royal Astronomical Society, 453, 1324, starbench: the D-type expansion of an H ii region

Capriotti E. R., Kozminski J. F., 2001, Publications of the Astronomical Society of the Pacific, 113, 677, Relative Effects of Ionizing Radiation and Winds from O-Type Stars on the Structure and Dynamics of H ii Regions

Dyson J. E., 1977, Astronomy and Astrophysics, 59, 161, Stellar wind bubbles in H II regions

Ekström S., et al., 2012, Astronomy & Astrophysics, 537, A146, Grids of stellar models with rotation

Ferland G. J., et al., 2017, Revista Mexicana de Astronomia y Astrofisica, 53, 385, The 2017 Release Cloudy

Geen S., Rosdahl J., Blaizot J., Devriendt J., Slyz A., 2015, Monthly Notices of the Royal Astronomical Society, 448, 3248, A detailed study of feedback from a massive star

Geen S., Watson S. K., Rosdahl J., Bieri R., Klessen R. S., Hennebelle P., 2018, Monthly Notices of the Royal Astronomical Society, 481, 2548, Chaos, Stochasticity, and the Unpredictability of Star Formation on a Cloud Scale

Geen S., Pellegrini E., Bieri R., Klessen R., 2019, Monthly Notices of the Royal Astronomical Society, p. 3101, When HiiRegions are Complicated: Considering Perturbations from Winds, Radiation Pressure, and Other Effects

Götberg Y., de Mink S., Groh J., Leitherer C., Norman C., 2019, Astronomy & Astrophysics, 629, A134, The impact of stars stripped in binaries on the integrated spectra of stellar populations

Heger A., Fryer C. L., Woosley S. E., Langer N., Hartmann D. H., 2003, The Astrophysical Journal, 591, 288, How Massive Single Stars End Their Life

Krumholz M. R., Matzner C. D., 2009, The Astrophysical Journal, 703, 1352, The Dynamics of Radiation-Pressure-Dominated HII Regions

Leitherer C., Ekström S., Meynet G., Schaerer D., Agienko K. B., Levesque E. M., 2014, The Astrophysical Journal Supplement Series, 212, 14, The Effects Of Stellar Rotation. II A Comprehensive Set of STARBURST99 Models

Maxwell M., Stefano D., 2017, 230, Mind you Ps and Qs: The interrelation between Period (P) and Mass-ratio (Q) Distributions of Binary Stars

Pabst C., et al., 2019, Nature, Volume 565, Issue 7741, p.618-621, 565, 618, Disruption of the Orion Molecular Core 1 by the stellar wind of the massive star Theta 1 Ori C

Rahner D., Pellegrini E. W., Glover S. C. O., Klessen R. S., 2017, Monthly Notices of the Royal Astronomical Society, 470, 4453, Winds and radiation in unison: a new semi-analytic feedback model for cloud dissolution

Rosdahl J., Blaizot J., Aubert D., Stranex T., Teyssier R., 2013, Monthly Notices of the Royal Astronomical Society, 436, 2188, RAMSES-RT: radiation hydrodynamics in the cosmological context

Sana H., et al., 2012, Science, 337, 444, Binary interaction dominates the evolution of massive stars

Spitzer L., 1978, Physical processes in the interstellar medium. New York Wiley-Interscience

Thornton K., Gaudlitz M., Janka H.-Th., Steinmetz M., 1998, The Astrophysical Journal, 500, 95, Energy Input and Mass Redistribution by Supernovae in the Interstellar Medium

Weaver R., McCray R., Castor J., Shapiro P., Moore R., 1977, The Astrophysical Journal, 218, 377, Interstellar bubbles. II - Structure and evolution

Appendix

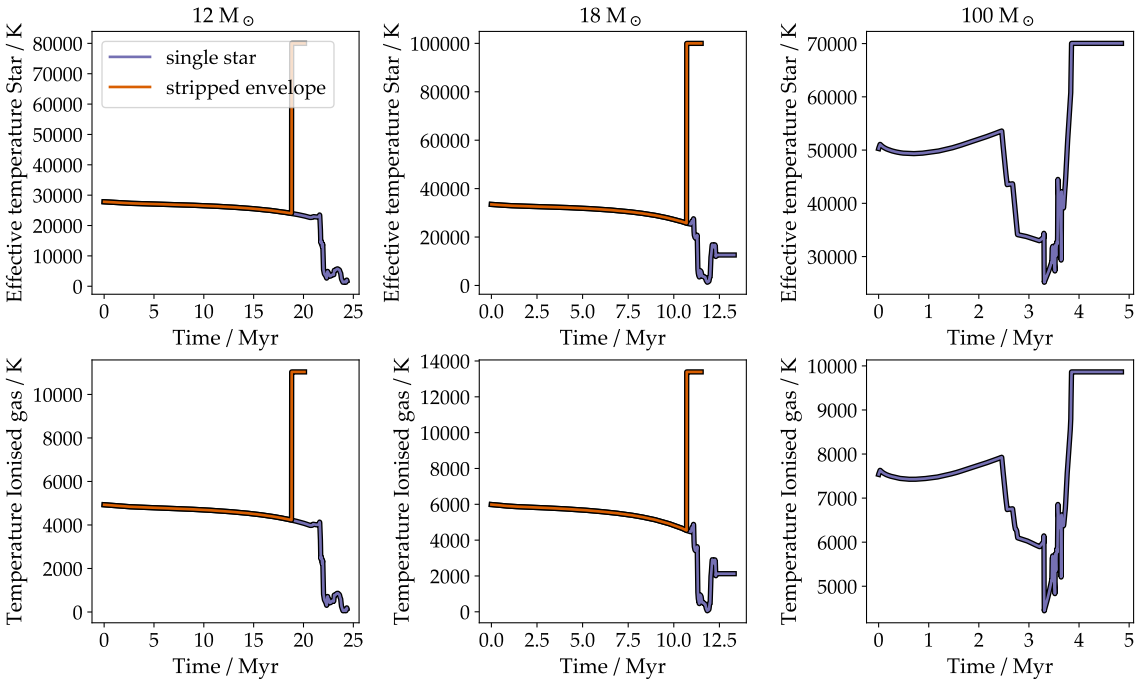

Figure 16: Effective temperature, temperature of the ionised gas of the envelope evolution and stellar track for the 12 $M_\odot$, 18 $M_\odot$ and 100 $M_\odot$ star.

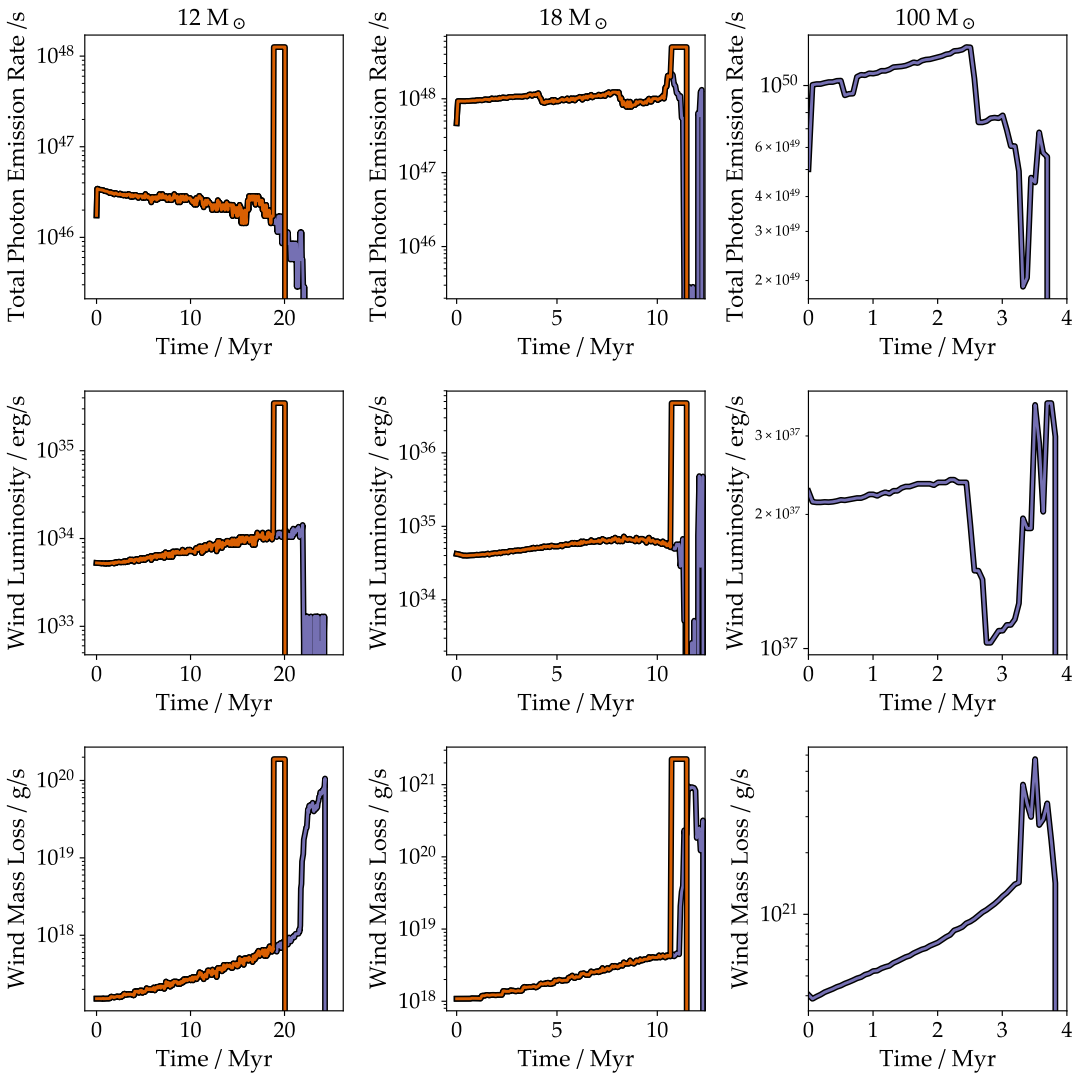

Figure 17: Total photon emission rate, wind luminosity and wind mass loss of the envelope evolution and stellar track for the 12 $M_\odot$, 18 $M_\odot$ and the 100 $M_\odot$ star.